TÜBİTAK

Turkish Journal of Agriculture and Forestry

http://journals.tubitak.gov.tr/agriculture/

Research Article

Turk J Agric For
(2015) 39: 652-662

doi:10.3906/tar-1406-170

Sensitivity of soil evaporation and reference evapotranspiration to climatic variables in South Korea

Mehmet AYDIN[1,*], Yeong-Sang JUNG[1], Jae E. YANG[1], Su-Jung KIM[2], Kyung-Dae KIM[3]

[1]Department of Biological Environment, Kangwon National University, Chuncheon, South Korea
[2]Department of Biological and Environmental Sciences, Dongguk University, Seoul, South Korea
[3]Gangwon Agricultural Research and Extension Service, Chuncheon, South Korea

Received: 30.06.2014 • **Accepted/Published Online:** 22.12.2014 • **Printed:** 30.09.2015

Abstract: The quantification of evapotranspiration and soil evaporation is crucial for agricultural water management. The FAO-56 Penman–Monteith and E-DiGOR models were used to compute reference evapotranspiration (*Eto*) and bare soil evaporation, respectively, at 17 meteorological stations of South Korea, from 1980 to 2009. The same soil parameters were assumed for all stations in order to compare actual soil evaporation (*Ea*) rates jointly dominated by atmospheric evaporative demand and soil water availability, as well as the size of rainfall events. The sensitivity of Penman–Monteith type equations to the major climatic variables was determined based on 1-year dataset. The long-term mean annual precipitation and *Eto* calculated at selected stations over the country were 1339.7 mm and 1087.1 mm, respectively. Precipitation showed noticeable interyear fluctuations, and the annual *Eto* increased gradually during the study period. A strong correlation between pan evaporation (*Epan*) and *Eto* was observed ($R = 0.808$, $P < 0.001$), based on daily data of 30 years. Similarly, a significant correlation between *Epan* and potential soil evaporation (*Ep*) was existent ($R = 0.622$, $P < 0.01$). The *Ep* rates were lower than the *Eto* rates ($Ep = 0.8 \times Eto$). The magnitude of *Ea*, as calculated with the model, reached a level of 63% of *Ep*. On the other hand, *Ea* accounted for 29.4% to 50.3% of the total precipitation over South Korea. Potential soil evaporation was more sensitive to net radiation, while reference evapotranspiration was mostly affected by the relative humidity. Wind speed was the less effective variable. The contribution of soil heat flux was negligible. The sensitivity of both *Ep* and *Eto* to the same climatic variables showed significant differences among seasons and locations. The aridity index ranged from 0.85 to 2.13, and all the study sites could be classified as humid areas. An aridity index of less than 1 appeared about once every 6 to 7 years, based on the station averages.

Key words: Aridity index, evapotranspiration, sensitivity, soil evaporation

1. Introduction

Evapotranspiration (*Et*) represents the major consumptive use of irrigation water and rainfall on agricultural land. Temporal changes in *Et* have profound implications for hydrologic processes, as well as for agricultural crop performance (Li et al., 2013). Soil evaporation (*Es*) within and outside the crop-growing season can be a significant component of *Et* (Burt et al., 2005). Therefore, the loss of water due to *Es* should be addressed in order to adopt feasible management practices for conserving water in the soil profile (Bittelli et al., 2008; Vanderborght et al., 2010; Xiao et al., 2011). On the other hand, potential evaporation from bare soil (hereafter, potential soil evaporation) is similar to evaporation from open-water surface, and it is independent of the soil water content. However, under natural conditions, the soil surface is usually not at or near saturation. Therefore, actual evaporation from bare soil (in brief, actual soil evaporation) is largely dependent on soil's water content, in addition to meteorological conditions (Gowing et al., 2006; Konukcu, 2007; Aydin et al., 2008). The accurate estimation of the evaporation from bare soil is critical in the physics of land-surface processes. However, the models dealing with *Es* have expressed the rate of water loss from cropped areas, rather than that from bare fields (Aydin et al., 2005).

Reference evapotranspiration (*Eto*) is used to represent the evaporative demand of the atmosphere for a grass reference evapotranspiring surface with abundant water supply, and it is usually estimated using different methods (Allen et al., 1998; Gao et al., 2012; Ngongondo et al., 2013). It is also important to identify the spatiotemporal trends of evaporation and evapotranspiration under the changing climate, for use in regional water resources planning (Wang et al., 2011, 2013; Terink et al., 2013; Ebrahimpour et al., 2014; Hosseinzadeh-Talaee et al., 2014; Xing et al., 2014). Therefore, many studies have been done for estimating *Eto*

* Correspondence: maydin08@yahoo.com

in South Korea, to contribute to water resources planning, irrigation schedule, and environmental management (i.e. Kim and Kim, 2008; Baba et al., 2013). Some of these studies are related to the impact of climate change on evaporative demand of the atmosphere. For example, Rim (2008) investigated the effects on *Eto* of climate change due to urbanization at different locations all over South Korea from 1970 to 2004. The author concluded that urbanization affected *Eto*, and increasing *Eto* trends were observed in the country during the study period. On the other hand, Rim (2010) emphasized that the yearly and monthly effects of urbanization on *Eto* were closely related to solar radiation, relative humidity, wind speed, and change in temperature. Lee and Park (2008) calculated daily-based *Eto* at 23 meteorological stations in South Korea for the period of 1997–2006. Choi et al. (2010) compared measured and model-based *Eto*, using weather data in Seoul, for a span of 29 years. However, to our knowledge, there are very limited data available on bare soil evaporation in South Korea.

On the other hand, sensitivity analysis is required to assess the impact of climatic variables on evaporation or evapotranspiration (Xie and Zhu, 2013; Tabari and Hosseinzadeh-Talaee, 2014; Xu et al., 2014). Several leading studies have assessed the parameter sensitivity for vegetation or open-water surfaces (McCuen, 1974; Saxton, 1975; Coleman and DeCoursey, 1976; Beven, 1979). Although many studies to determine the effects of climatic variables on evapotranspiration have been done for sensitivity analysis of the Penman–Monteith equation (Beven, 1979; Goyal, 2004; Gong et al., 2006; Estévez et al., 2009; Kwon and Choi, 2011; Huo et al., 2013), studies on the sensitivity of the same model for potential soil evaporation are rare in the literature (Aydın and Keçecioğlu, 2010). There are different methods for sensitivity analyses, and different spatial-temporal scales were used in previous studies (Beven, 1979; Goyal, 2004; Gong et al., 2006). Dimensionless sensitivity coefficients are widely used, based on the partial derivative of the dependent variable to the independent variables (Ambas and Baltas, 2012).

The purposes of this study were, therefore, to attempt a comparative study of reference evapotranspiration and potential soil evaporation in different areas of South Korea; to evaluate the impact of climatic variables, such as radiation, air temperature, relative humidity, and wind speed, on potential soil evaporation/reference evapotranspiration; and to calculate the actual soil evaporation, using predefined soil parameters.

2. Materials and methods

2.1. Model descriptions

2.1.1. Bare soil evaporation

Evaporation from bare soils can be estimated using the E-DiGOR model, which incorporates the quantification of runoff, drainage, actual soil evaporation, and soil water storage (Aydin, 2008; Aydın et al., 2014). Potential soil evaporation is commonly computed using the classical Penman–Monteith equation, with a surface resistance of zero (Allen et al., 1994; Wallace et al., 1999; Aydin et al., 2005):

$$E_p = \frac{\Delta(R_n - G_s) + 86.4\rho c_p \delta / r_a}{\lambda(\Delta + \gamma)}, \quad (1)$$

where E_p is the potential soil evaporation (mm day^{-1}), Δ is the slope of the saturated vapor pressure–temperature curve (kPa °C^{-1}), R_n is the net radiation (MJ m^{-2} day^{-1}), G_s is the soil heat flux (MJ m^{-2} day^{-1}), ρ is the air density (kg m^{-3}), c_p is the specific heat of air (kJ kg^{-1} °C^{-1} = 1.013), δ is the vapor pressure deficit of the air (kPa), r_a is the aerodynamic resistance (s m^{-1}), λ is the latent heat of vaporization (MJ kg^{-1}), γ is the psychrometric constant (kPa °C^{-1}), and 86.4 is the factor for conversion from kJ s^{-1} to MJ day^{-1}.

Incorporating relative humidity (see Eq. (A1) in Appendix A; on the journal's website) and aerodynamic resistance (Eq. (A3)) into Eq. (1) for a bare soil surface yields:

$$E_p = \frac{\Delta(R_n - G_s) + 0.1248\rho c_p u_2 e_s (1 - \frac{H}{100})}{\lambda(\Delta + \gamma)}, \quad (2)$$

where, u_2, e_s, and H are the wind speed (m s^{-1}) at 2.0 m height, the saturation vapor pressure (kPa), and relative humidity (%), respectively. The actual soil evaporation can then be calculated by the Aydin equation (Aydin et al., 2005; Aydın et al., 2014).

$$E_a = \frac{Log|\psi| - Log|\psi_{ad}|}{Log|\psi_{tp}| - Log|\psi_{ad}|} E_p \quad (3)$$

If $|\psi| \le |\psi_{tp}|$, then $E_a = E_p$ or $E_a / E_p = 1$.

For $|\psi| \ge |\psi_{ad}|$, $E_a = 0$.

Note that $E_p \ge 0$.

Here, E_a is the actual soil evaporation (mm day^{-1}); $|\psi_{tp}|$ is the absolute value of soil water potential (matric potential) at which actual evaporation starts to drop below the potential one (cm of water); $|\psi_{ad}|$ is the absolute value of soil water potential at air-dryness (cm), which can be defined as the water potential of the soil dried to an air-dry state; and $|\Psi|$ is the absolute value of the soil water potential at the surface layer (cm). ψ_{tp} is closely related to soil texture. Similarly, Ψ is a function of flow path tortuosity, the volumetric water content at field capacity, soil water depletion, and hydraulic diffusivity which are

also related to soil texture (see Aydin et al., 2008; Aydın et al., 2014).

2.1.2. Reference evapotranspiration

The Penman–Monteith method, considering aerodynamic resistance and surface resistance, has been successfully used to calculate evapotranspiration from different land covers (Gao et al., 2012). According to Allen et al. (1998), the Penman–Monteith combination method may be simplified to estimate the evapotranspiration rate from a reference crop (i.e. clipped grass) by assuming constants for some parameters. For simplicity, a crop height is set at 0.12 m, with a fixed surface resistance of 70 s m^{-1} and an albedo of 0.23. The aerodynamic resistance is calculated as a function of wind speed (i.e. $r_a = 208/u_2$). Consequently, the FAO-56 Penman–Monteith (hereafter, FAO56-PM) equation (Allen et al., 1998) may be written as:

$$Et_O = \frac{0.408\Delta(R_n - G_s) + \gamma \frac{900}{T_a + 273} u_2 e_s \left(1 - \frac{H}{100}\right)}{\Delta + \gamma(1 + 0.34u_2)}, \quad (4)$$

where Et_O is the grass reference evapotranspiration (mm day^{-1}), and T_a is the mean daily air temperature (°C). Since the magnitude of daily soil heat flux beneath the grass reference surface is relatively small, G_s can be ignored (Allen et al., 1998).

2.1.3. Sensitivity analysis

There are different ways to compute sensitivity coefficients for climatic variables (Goyal, 2004; Gong et al., 2006; Irmak et al., 2006; Estévez et al., 2009; Huo et al., 2013). In this study, the nondimensional relative sensitivity coefficients were calculated following McCuen (1974) and Beven (1979):

$$S_i = \frac{\partial O}{\partial V_i} \cdot \frac{V_i}{O}, \quad (5)$$

where S_i represents the fraction of change in variable V_i, transmitted to the change in output O. The derived formulas for the relative sensitivity coefficients are given in Appendix B (on the journal's website).

2.2. Study locations and data source

In this research, 17 meteorological stations were selected across South Korea (Table). Daily climate data were collected from the meteorological stations for the period of 1980–2009. In addition, for some comparisons, 30 years' worth of pan evaporation data (from April to October) were obtained from one station (Chuncheon). South Korea has a humid continental and a humid subtropical climate, with 4 distinct seasons and a wide temperature difference between summer and winter. The annual precipitation on the mainland ranges from about 1000 to 1500 mm.

Table. Coordinates of the selected meteorological stations.

Station no.	Station name	Latitude (N)	Longitude (E)	Elevation (m)
100	Daegwallyeong	37°40′	128°43′	772.4
101	Chuncheon	37°54′	127°44′	76.8
105	Gangneung	37°45′	128°53′	26.1
108	Seoul	37°34′	126°57′	85.5
112	Incheon	37°28′	126°37′	69.0
119	Suwon	37°16′	126°59′	34.5
129	Seosan	36°46′	126°29′	25.2
131	Cheongju	36°38′	127°26′	56.4
133	Daejeon	36°22′	127°22′	62.6
136	Andong	36°34′	128°42′	140.7
138	Pohang	36°01′	129°22′	1.3
143	Daegu	35°53′	128°37′	57.3
146	Jeonju	35°49′	127°09′	61.0
159	Busan	35°06′	129°01′	69.2
165	Mokpo	34°49′	126°22′	37.4
184	Jeju	33°30′	126°31′	19.9
192	Jinju	35°09′	128°02′	27.1

Most soils are derived from granite and gneiss. Sandy and brown-colored soils with low organic matter content are common.

Unlike the potential soil evaporation (*Ep*), the actual soil evaporation (*Ea*) is largely influenced by soil wetness. In other words, the magnitude of *Ea* is strongly related to temporal rainfall pattern, because the contribution of rainfall to soil water content is considerably dependent on the size of rainfall events. Thus, in the calculations, the same soil properties were assumed for all locations to compare *Ep* and *Ea* rates under different climatic conditions, as suggested by Onder et al. (2009). The FAO56-PM equation was applied to determine the daily reference evapotranspiration during the period of 1980–2009. Potential and actual evaporations from bare soil were calculated, using the E-DiGOR computer program (Aydin, 2008; Aydın and Polat, 2010). Simulations were done for a sandy loam soil with a nearly level, bare surface. The measured and nonmeasured parameters of the defined soil were obtained from the literature (van Dam et al., 1997; Ács, 2003; Moret et al., 2007; Aydin et al. 2012). The sensitivity analyses of the Penman–Monteith type equations to the major climatic elements were carried out for a single year, because they require a large number of computations. The nondimensional relative sensitivity coefficients, as defined by Eqs. (B1)–(B10), were calculated on a daily basis for net radiation, air temperature, relative humidity, and wind speed using climatic data of 2009 (from March to October). Monthly average sensitivity coefficients were obtained by averaging daily values. Representative regional sensitivity coefficients (Gong et al., 2006) were determined by averaging the values of the stations located in similar geographical positions (mountain, inland, and coastal area).

3. Results

The magnitudes of annual precipitation, reference evapotranspiration (*Eto*), and potential (*Ep*) and actual (*Ea*) soil evaporations are compared in Figure 1 for different stations of South Korea. In most locations, the 30-year (hereafter, long-term) mean annual precipitation was higher than *Eto*. Long-term mean annual precipitation varied from 1064 to 1835 mm. Nevertheless, of all the locations, the southeastern coastal areas had the largest amount of annual precipitation, at or around 1500 mm, because the summer monsoon front approaches the Korean Peninsula from the south. Thus, significant rainfall occurs in summer (June through August). The

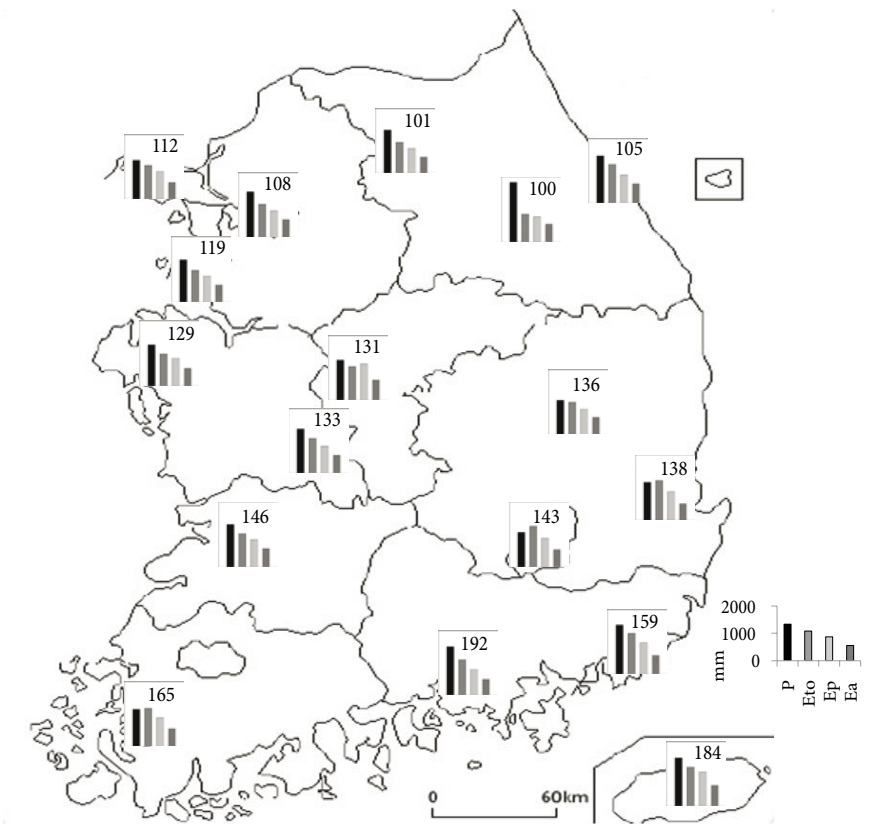

Figure 1. The histograms for long-term (30-year) mean annual precipitation (*P*), reference evapotranspiration (*Eto*), and potential (*Ep*) and actual (*Ea*) soil evaporation at labeled meteorological stations in South Korea (the legend shows the average of the stations).

spatial pattern of *Eto* showed high evaporative demand of the atmosphere in the southeastern coastal and adjacent areas, as well as at eastern coastal stations. In contrast, the lowest *Eto* rates were found in the northern part. The rates of *Eto* were greater than those of *Ep* at all stations, except Cheongju (station 131). However, the spatial distribution of *Ep* was usually consistent with that of *Eto*. The annual *Ep* was always greater than *Ea*, because *Ea* is dependent not only on the atmospheric conditions but also on soil wetness and, consequently, soil water potential.

The relation between *Epan* and *Eto*, as well as the potential soil evaporation (*Ep*), was demonstrated using the 30-year daily data (from April to October) from Chuncheon (station 101) as an example (Figure 2). The

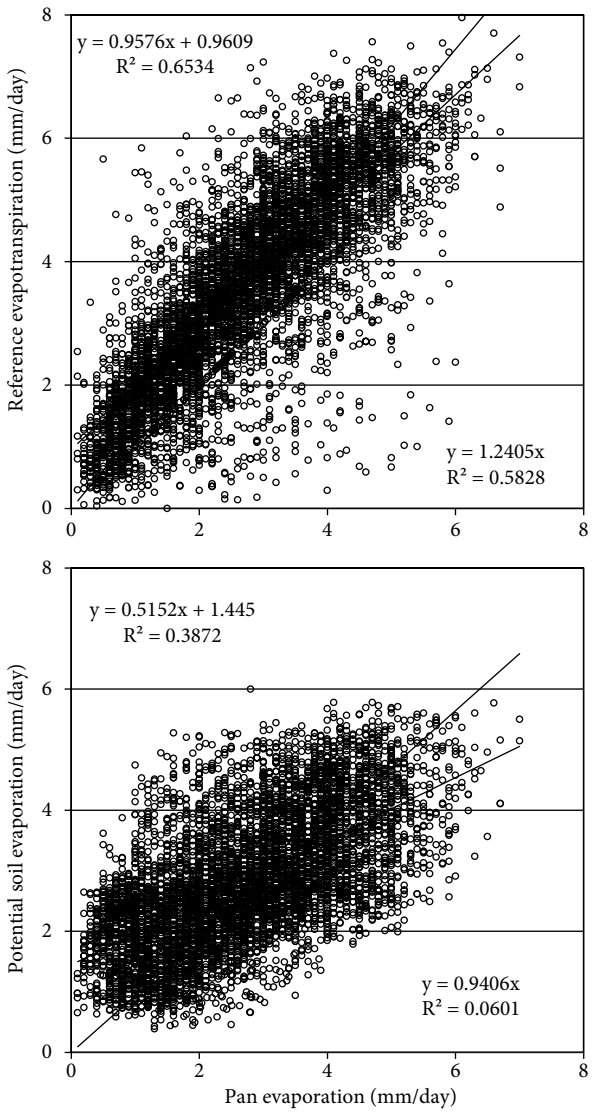

Figure 2. The relation between observed pan evaporation and calculated reference evapotranspiration/potential soil evaporation, based on the data of 1980 to 2009.

linear regressions with and without an intercept are provided on the charts. A strong correlation between *Epan* and *Eto* was observed ($R = 0.808$, $P < 0.001$). On the other hand, the correlation between *Epan* and calculated *Ep* was weaker, but still significant ($R = 0.622$, $P < 0.01$).

In order to determine the adequacy of precipitation in satisfying the evaporative demand of the atmosphere, the aridity index (*AI*) was calculated (Figure 3). This index is usually defined as the ratio of precipitation to potential evapotranspiration (UNESCO, 1979; Badini et al., 1997; Wolfe, 1997). Variations of annual precipitation and *Eto* during a 30-year period across South Korea are shown in Figure 4. The annual precipitation denoted noticeable interannual fluctuations, while the annual *Eto* increased gradually. An aridity index of less than 1 was observed about once every 6 or 7 years and was associated with lower precipitation (e.g., in 1982, 1988, 1994, 2001, and 2008), based on the average of the stations. The relationship between precipitation and the ratio of actual soil evaporation to precipitation (*Ea/P*) is demonstrated in Figure 5. A negative linear relationship between *Ea/P* and precipitation was obtained. In other words, the ratio of evaporative water loss to precipitation has demonstrated that a higher percentage of total rain water will be lost through soil evaporation in drier years.

The sensitivity analysis of the Penman–Monteith type equations to the major climatic variables was performed for 2009 only. Daily average rates of *Ep* were lower than those of *Eto* in all geographical locations and seasons (Figure 6). The sensitivity coefficients of key climatic variables are given in Figures 7 and 8. For example, a sensitivity coefficient of 0.3 for a climatic variable would suggest that a 20% increase of that variable, while the other variables are held constant, may also increase a dependent variable (*Ep* or *Eto*) by 6%. Negative coefficients would indicate that a reduction in a dependent variable would result from an increase in that climatic variable.

4. Discussion

On average, the long-term mean annual precipitation and *Eto* across the country were 1339.7 and 1087.1 mm, respectively. These results were the average value of all 17 stations, giving a good geographical representation of the country (Figure 1). On the other hand, the rates of *Ep* were lower than those of *Eto* ($Ep = 0.8 \times Eto$), based on the average of all stations. Similar relationships between *Ep* and *Eto* can be found in the literature (Kroes et al., 1999; Aydin et al., 2008; Aydın et al., 2012). The annual *Ep* was greater than *Ea*, because *Ea* is largely influenced by the contribution of rainfall to soil water content and, consequently, by the soil wetness. Less frequent rainfall may result in less evaporative loss; therefore, the size of rainfall events may account for a portion of the variations

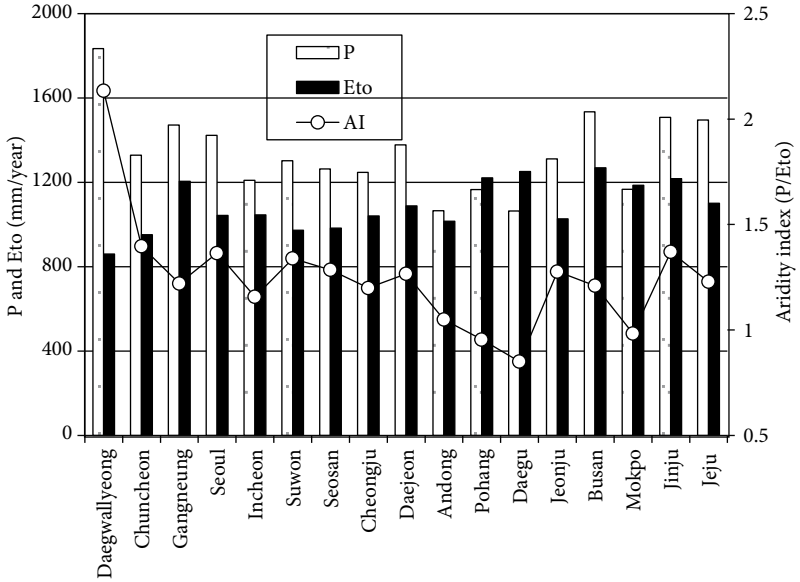

Figure 3. Long-term mean annual precipitation (*P*), reference evapotranspiration (*Eto*), and aridity index (AI) for corresponding stations.

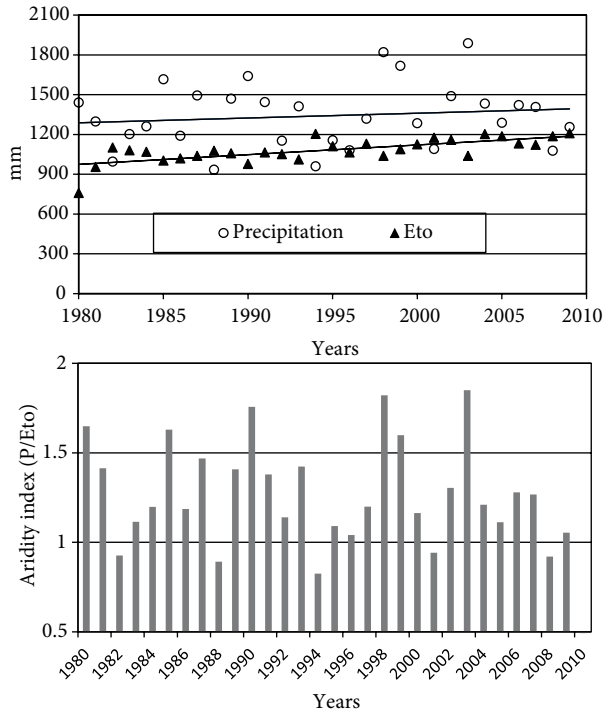

Figure 4. Changes in precipitation, reference evapotranspiration, and aridity index across South Korea from 1980 to 2009.

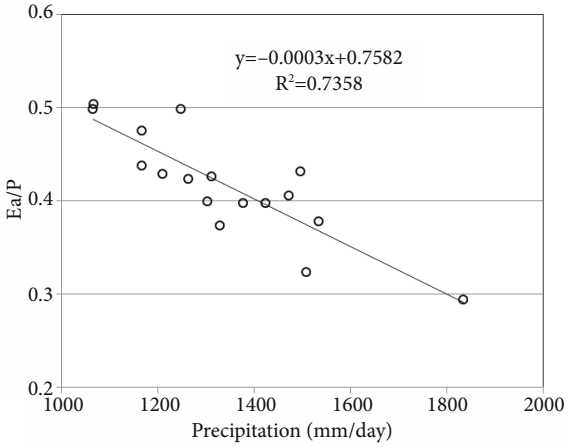

Figure 5. The relation between precipitation and the ratio of actual soil evaporation to precipitation (*Ea/P*) in South Korea, based on mean data of 30 years.

in actual soil evaporation. In other words, *Ea* is jointly dominated by atmospheric evaporative power and soil water content, as well as by temporal rainfall pattern. Similarly, Gao et al. (2007) reported that in most parts of China, the change in precipitation played a key role in the change of estimated actual evapotranspiration.

On the basis of linear regression without intercept, the FAO56-PM model overestimated reference evapotranspiration by an average 24%, in comparison with the daily pan measurements of 30 years (Figure 2). Some previous studies have indicated that *Eto* results differed quite strongly depending on the model used. For example, Hosseinzadeh-Talaee et al. (2014) concluded that *Eto* estimated by the Hargreaves model was about 19% lower compared to *Epan*. Some other results showed that Penman–Monteith-based models (FAO56-PM and ASCE-PM) significantly overestimated the evapotranspiration

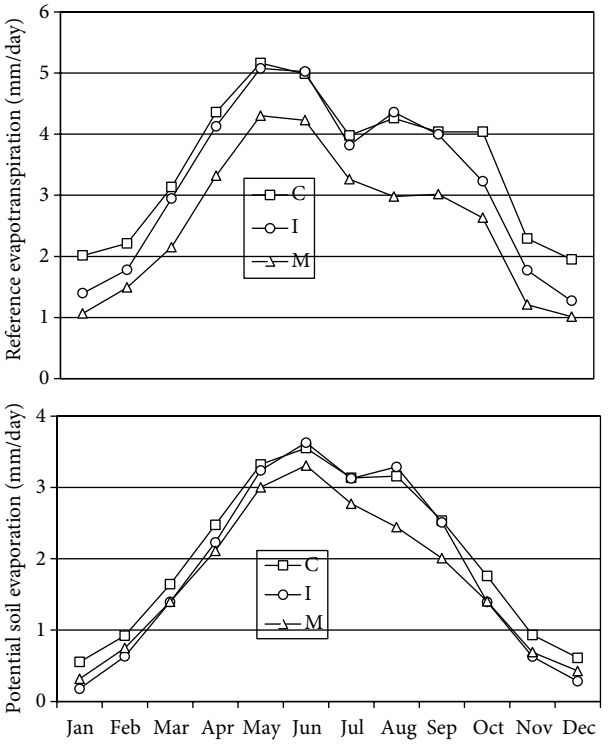

Figure 6. Changes in reference evapotranspiration and potential soil evaporation in different geographical locations (C: coastal area, I: inland, M: mountain) of South Korea in 2009.

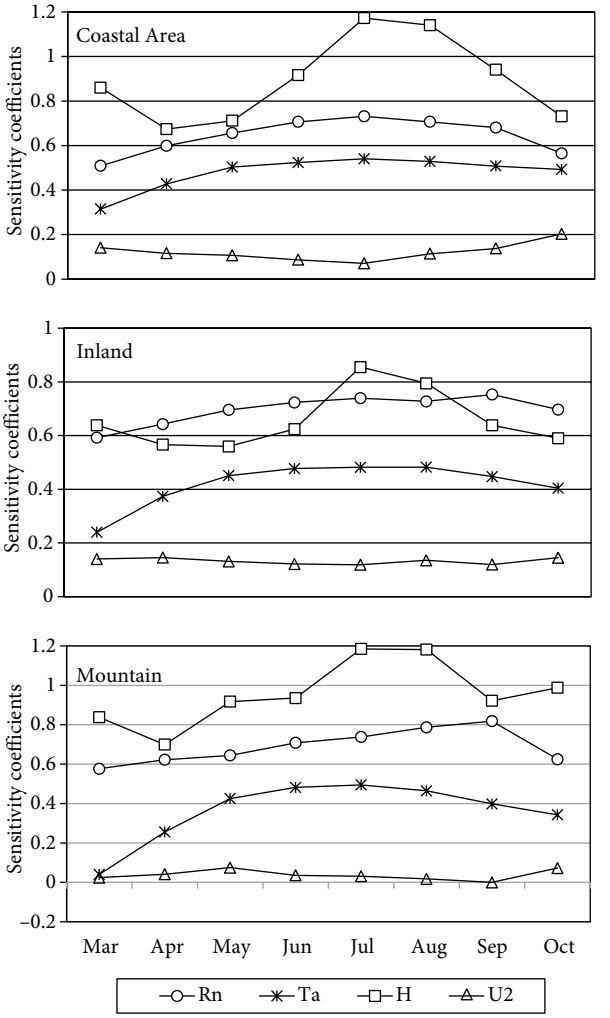

Figure 7. Daily averaged sensitivity coefficients for net radiation (Rn), air temperature (Ta), relative humidity (H), and wind speed (u_2) transmitted to *Eto* in 2009 (the coefficients for H were multiplied by –1 to facilitate visual comparison).

compared to the Hargreaves, Priestley–Taylor, and Thornthwaite approaches (Herrnegger et al., 2012; Ngongondo et al., 2013). Several factors, such as the radiation reflection from the surfaces, heat storage and transfer within and/or through the sides of media, differences in turbulence, or temperature and humidity of the air immediately above the respective surfaces, may produce obvious differences in loss of water from a water surface and from a cropped surface (Allen et al., 1998). Moreover, crop height and leaf area index parameters may result in considerable deviations. In addition, pan evaporation measurements during rainy days may have some inaccuracy. As can be seen in Figure 2, *Eto* has a much stronger correlation with *Epan*, while the correlation between *Ep* and *Epan* is much weaker. The pan position and its environment (the ground cover of the station and its surroundings) have a significant influence on the measured results of pan evaporation (Allen et al., 1998). Since the pan is located on a short green (grass) cover in the study station, it is therefore reasonable to expect a better correlation between *Eto* and *Epan*.

The long-term mean annual precipitation was higher than *Eto* in most locations, except Pohang (station 138), Daegu (station 143), and Mokpo (station 165). The aridity index (*AI*) ranged from 0.85 (Daegu) to 2.13 (Daegwallyeong), and all study locations can be classified as humid areas based on the UNESCO (1979) classification. Furthermore, obvious differences among the years appeared in terms of *AI* (Figures 3 and 4). Therefore, in such studies, a correction is needed to amend the mismatch between long- and short-term data. The annual precipitation was likely to increase according to the trend line, although it denoted noticeable interannual fluctuations. The annual *Eto* increased gradually (Figure 4). According to Im et al. (2012), significant warming is found in future projections regardless of the season and region, while the change in precipitation shows a mixed feature, with both increasing and decreasing patterns in South Korea. Their result indicates that under global warming, without an increase in precipitation appropriate for the

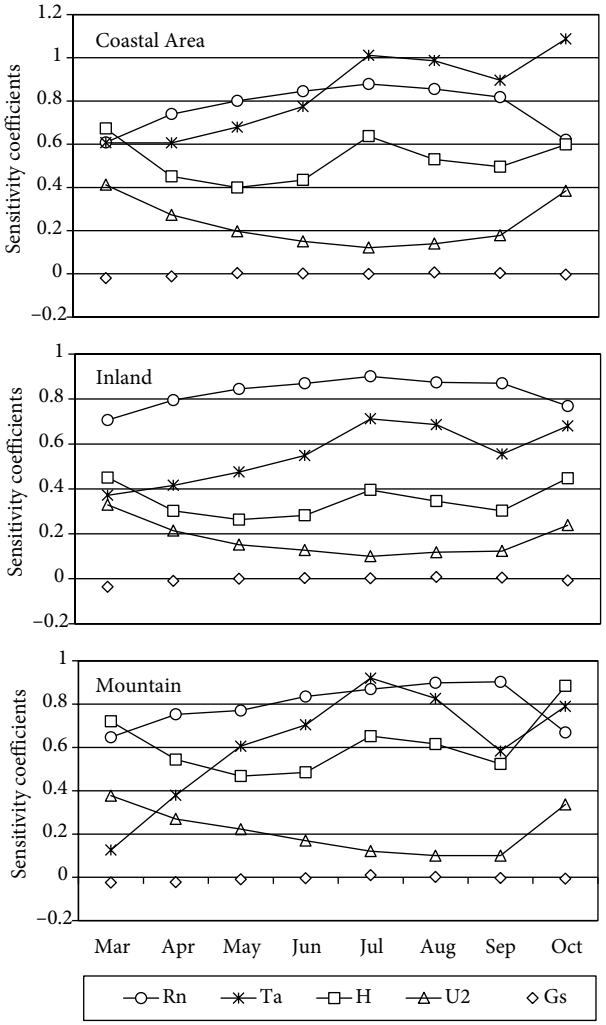

Figure 8. Daily averaged sensitivity coefficients for net radiation (Rn), air temperature (Ta), relative humidity (H), wind speed (u_2), and soil heat flux (Gs) transmitted to *Ep* in 2009 (the coefficients for H were multiplied by –1 to facilitate visual comparison).

evaporative demand of the atmosphere, future dryness is a more likely condition. Some other studies have raised similar concerns about the water resources and agriculture in South Korea (Boo et al., 2004; Kim et al., 2005; Kyoung et al., 2011; Oh et al., 2011; Yoo et al., 2012).

Initially, evaporation from a wet soil proceeds at the potential rate. That is to say, as much soil water is lost as the atmosphere allows. When the soil surface becomes drier, water cannot be supplied from deeper layers to the soil surface fast enough to meet the higher evaporative demand of the atmosphere (Konukcu et al., 2004; Aydin et al., 2005), even in rainy seasons. The rate of actual soil evaporation is therefore limited by atmospheric evaporative demand and soil properties. The actual soil evaporation, as calculated with the model, accounted for 29.4% to 50.3% of the total precipitation (Figure 5).

These results, without any validation, may not allow such a clear-cut conclusion; however, the credibility of the E-DiGOR model has been demonstrated by different researchers, using field-based measurements in a wide range of environments, in Japan and Turkey (Aydin et al., 2005, 2008; Aydin, 2008; Kurt, 2011).

The seasonal variations of *Eto* and *Ep* in different geographical locations revealed similar patterns (Figure 6). On the other hand, both *Ep* and *Eto* at the station on the mountain (station 100) were lower than those in coastal areas (stations 105, 112, 129, 138, 159, 165, 184, and 192) and inland (stations 101, 108, 119, 131, 133, 136, 143, and 146). In general, potential soil evaporation was more sensitive to net radiation, while reference evapotranspiration was mostly affected by relative humidity. This is consistent with findings of Wang et al. (2012), who recognized that relative humidity was always the most sensitive variable to *Eto* across the Yellow River Basin, but sometimes not the dominant factor in *Eto* change. Wind speed was the least sensitive variable in both *Eto* and *Ep* (Figures 7 and 8). Similarly, Gong et al. (2006), analyzing the sensitivity of the FAO56-PM model, found lower sensitivity coefficients for wind speed throughout the year in the Yangtze River Basin of China. However, Huo et al. (2013) reported that, for *Eto*, wind speed was the most sensitive meteorological variable, followed by relative humidity, temperature, and radiation in an arid-inland region of China. According to Dinpashoh et al. (2011), the ubiquitous windy conditions in dry regions (which, by the way, does not apply to the present study region) may have had a dominant influence on the observed *Eto* changes. In contrast, Goyal (2004) emphasized that *Eto* was sensitive to temperature and net solar radiation, followed by wind speed and vapor pressure, in an arid region of India. In the present study, the contribution of soil heat flux to evaporation was negligible; it was not considered in the sensitivity analysis of *Eto*. The response of both *Ep* and *Eto* to the same climatic variables showed considerable differences among seasons. The order of the variables was changing in some locations. Li et al. (2013) stated that the wind speed, relative humidity, and maximum temperature were the most causative variables for the change of *Eto* in the Heihe River Basin of China. From seasonal and spatial perspectives, the order of their contributions was different. Estévez et al. (2009) also reported that the sensitivity of evapotranspiration (or evaporation) to the same climatic variables varied with location. Tabari and Hosseinzadeh-Talaee (2014) indicated that the order of sensitivity coefficients changed with aridity or humidity of the environments.

As discussed above, contradicting results can be found in the literature. In our study, reference evapotranspiration was more sensitive to relative humidity in the coastal areas and the mountains, followed by radiation, air temperature,

and wind speed (Figure 7). This order of sensitivity coefficients is similar to that reported by Gong et al. (2006). However, Kwon and Choi (2011) found that in Korea, vapor pressure had the most influence on *Eto*, followed by wind speed and radiation. In inland stations of this study, radiation and relative humidity were the main parameters that affected evapotranspiration. In general, *Ep* was more sensitive to net radiation, followed by air temperature, relative humidity, and wind speed (Figure 8). The results for *Ep* are not directly comparable to those of previous works, due to the differences of the equations being utilized, of the study media, of the varied approaches to conducting the sensitivity analyses, and of the derived and defined sensitivity coefficients (Estévez et al., 2009). Some other studies (McCuen, 1974; Saxton, 1975; Coleman and DeCoursey, 1976; Beven, 1979) showed that potential evaporation (or evapotranspiration) was much more sensitive to radiation, humidity, and temperature. Although there are differences in the sensitivity of soil evaporation and evapotranspiration to net radiation, it is clear that net radiation is the most important variable at the study locations. For example, net radiation was the most sensitive variable to *Ep*, and it was the second most sensitive variable to *Eto*. This means that latent heat flux plays a major role in the dissipation of the net radiation (Agam et al., 2004) in the studied region. In other words, evaporation/evapotranspiration plays not only a key role in the energy balance in the earth's atmospheric system, but it is also an essential element of water balance (Wang et al., 2012).

In order to explain the reasons for the sensitivity of *Eto* and *Ep* to different climatic variables, the influence of surface types on these processes should be considered. Differences in radiation reflection (an albedo of 0.23 and 0.15 for grass and soil surfaces, respectively), heat storage and transfer of the media (daily soil heat flux is ignored for grass land, but may sometimes be important for bare soil), aerodynamic resistance above surfaces (i.e. $r_a = 208/u_2$ for grass and $r_a = 692.1/u_2$ for soil), surface resistance (70 s m^{-1} for grass and negligible for soil), leaf area index, and so on may produce obvious differences in loss of water from cropped land and from bare soil. These factors may explain why *Eto* and *Ep* are sensitive to the different climatic variables and why the sensitivity coefficients change seasonally and geographically. In addition, the sensitivity coefficients vary day-by-day, being dependent on the current value of all the independent variables and the dependent variable.

In conclusion, the reference evapotranspiration (*Eto*) increased during the study period. The actual soil evaporation (*Ea*) reached a level of 63% of potential soil evaporation (*Ep*), based on the country average. However, the impacts of different soil types on evaporation at farm-scale level could be offset by using local soil characteristics. For *Ep*, net radiation was the most sensitive variable; however, for *Eto*, relative humidity was the most influential variable. Wind speed was the least effective variable for both *Eto* and *Ep*, and soil heat flux could not be considered in the sensitivity analysis. The sensitivity coefficients calculated on a daily basis may not reflect the site-specific conditions; therefore, monthly average coefficients may accommodate the features of the locations. These results can provide beneficial references for agricultural water management, irrigation practices, and crop production in South Korea. Concurrently, we can understand what the possible implications of climate change would be for soil water balance.

Acknowledgment

This study was carried out with the basic research support of Kangwon National University in 2013.

References

Ács F (2003). A comparative analysis of transpiration and bare soil evaporation. Bound-Lay Meteorol 109: 139–162.

Agam N, Berliner PR, Zangvil A, Ben-Dor E (2004). Soil water evaporation during the dry season in an arid zone. J Geophys Res-Atmos 109: D16103.

Allen RG, Pereira LS, Raes D, Smith M (1998). Crop Evapotranspiration: Guidelines for Computing Crop Water Requirements. Irrigation and Drainage Paper No. 56. Rome, Italy: FAO.

Allen RG, Smith M, Perrier A, Pereira LS (1994). An update for the definition of reference evapotranspiration. ICID Bulletin 43: 92.

Ambas VT, Baltas E (2012). Sensitivity analysis of different evapotranspiration methods using a new sensitivity coefficient. Global NEST J 14: 335–343.

Aydin M (2008). A model for evaporation and drainage investigations at ground of ordinary rainfed-areas. Ecol Model 217: 148–156.

Aydın M, Jung YS, Yang JE, Lee HI (2014). Long-term water balance of a bare soil with slope in Chuncheon, South Korea. Turk J Agric For 38: 80–90.

Aydin M, Jung YS, Yang JE, Lee HI, Kim KD (2012). Simulation of soil hydrological components in Chuncheon over 30 years using E-DiGOR model. Korean J Soil Sci Fert 45: 484–491.

Aydın M, Keçecioğlu SF (2010). Sensitivity analysis of evaporation module of E-DiGOR model. Turk J Agric For 34: 497–507.

Aydın M, Polat V (2010). A computer program for E-DiGOR model. In: Proceedings of the International Soil Science Congress on Management of Natural Resources to Sustain Soil Health and Quality, 26–28 May 2010; Samsun, Turkey: pp. 9–16.

Aydin M, Yang SL, Kurt N, Yano T (2005). Test of a simple model for estimating evaporation from bare soils in different environments. Ecol Model 182: 91–105.

Aydin M, Yano T, Evrendilek F, Uygur V (2008). Implications of climate change for evaporation from bare soils in a Mediterranean environment. Environ Monit Assess 140: 123–130.

Baba APA, Shiri J, Kisi O, Fard AF, Kim S, Amini R (2013). Estimating daily reference evapotranspiration using available and estimated climatic data by adaptive neuro-fuzzy inference system (ANFIS) and artificial neural network (ANN). Hydrol Res 44: 131–146.

Badini O, Stockle CO, Franz ED (1997). Application of crop simulation modelling and GIS to agroclimatic assessment in Burkina Faso. Agr Ecosyst Environ 64: 233–244.

Beven K (1979). A sensitivity analysis of the Penman–Monteith actual evapotranspiration estimates. J Hydrol 44: 169–190.

Bittelli M, Ventura F, Campbell GS, Snyder RL, Gallegati F, Pisa PR (2008). Coupling of heat, water vapor, and liquid water fluxes to compute evaporation in bare soils. J Hydrol 362: 191–205.

Boo KO, Kwon WT, Oh JH, Baek HJ (2004). Response of global warming on regional climate change over Korea: An experiment with the MM5 model. Geophys Res Lett 31: L21206.

Burt CM, Mutziger AJ, Allen RG, Howell TA (2005). Evaporation research: review and interpretation. J Irrig Drain Eng 131: 37–58.

Choi W, Choi M, Oh H, Park J (2010). Estimation on trends of reference evapotranspiration of weather station using Reference Evapotranspiration Calculator Software. KSCE Journal of Civil Engineering 30: 219–231.

Coleman G, DeCoursey DG (1976). Sensitivity and model variance analysis applied to some evaporation and evapotranspiration models. Water Resour Res 12: 873–879.

Dinpashoh Y, Jhajharia D, Fakheri-Fard A, Singh VP, Kahya E (2011). Trends in reference crop evapotranspiration over Iran. J Hydrol 399: 422–433.

Ebrahimpour M, Ghahreman N, Orang M (2014). Assessment of climate change impacts on reference evapotranspiration and simulation of daily weather data using SIMETAW. J Irrig Drain Eng 140: 04013012.

Estévez J, Gavilán P, Berengena J (2009). Sensitivity analysis of a Penman–Monteith type equation to estimate reference evapotranspiration in southern Spain. Hydrol Process 23: 3342–3353.

Gao G, Chen D, Xu CY, Simelton E (2007). Trend of estimated actual evapotranspiration over China during 1960-2002. J Geophys Res-Atmos 112: D11120.

Gao G, Xu CY, Chen D, Singh VP (2012). Spatial and temporal characteristics of actual evapotranspiration over Haihe River basin in China estimated by the complementary relationship and the Thornthwaite water balance model. Stoch Env Res Risk A 26: 655–669.

Gong L, Xu C, Chen D, Halldin S, Chen YD (2006). Sensitivity of the Penman–Monteith reference evapotranspiration to key climatic variables in the Changjiang (Yangtze River) basin. J Hydrol 329: 620–629.

Gowing JW, Konukcu F, Rose DA (2006). Evaporative flux from a shallow watertable: The influence of a vapour–liquid phase transition. J Hydrol 321: 77–89.

Goyal RK (2004). Sensitivity of evapotranspiration to global warming: a case study of arid zone of Rajasthan (India). Agric Water Manage 69: 1–11.

Herrnegger M, Nachtnebel HP, Haiden T (2012). Evapotranspiration in high alpine catchments - an important part of the water balance! Hydrol Res 43: 460–475.

Hosseinzadeh-Talaee P, Tabari H, Abghari H (2014). Pan evaporation and reference evapotranspiration trend detection in western Iran with consideration of data persistence. Hydrol Res 45: 213–225.

Huo Z, Dai X, Feng S, Kang S, Huang G (2013). Effect of climate change on reference evapotranspiration and aridity index in arid region of China. J Hydrol 492: 24–34.

Im ES, Ahn JB, Kim DW (2012). An assessment of future dryness over Korea based on the ECHAM5-RegCM3 model chain under A1B emission scenario. Asia-Pac J Atmos Sc 48: 325–337.

Irmak S, Payero JO, Martin DL, Irmak A, Howell TA (2006). Sensitivity analyses and sensitivity coefficients of standardized daily ASCE Penman–Monteith equation. J Irrig Drain Eng 132: 564–578.

Kim S, Kim HS (2008). The integrational operation method for the modeling of pan evaporation and the alfalfa reference evapotranspiration. KSCE Journal of Civil Engineering 28: 199–213.

Kim YO, Seo YW, Lee DR, Yoo C (2005). Potential effects of global warming on a water resources system in Korea. Water Int 30: 400–405.

Konukcu F (2007). Modification of the Penman method for computing bare soil evaporation. Hydrol Process 21: 3627–3634.

Konukcu F, Istanbulluoglu A, Kocaman I (2004). Determination of water content in drying soils: incorporating transition from liquid phase to vapour phase. Aust J Soil Res 42: 1–8.

Kroes JG, van Dam JC, Huygen J, Vervoort RW (1999). User's Guide of SWAP Version 2.0. Technical Document 53, DLO WSC Report 81. Wageningen, the Netherlands: Department of Water Resources, Wageningen Agricultural University.

Kurt N (2011). Monitoring of soil water budget using E-DiGOR model in olive producing area. PhD, Mustafa Kemal University, Hatay, Turkey.

Kwon H, Choi M (2011). Error assessment of climate variables for FAO-56 reference evapotranspiration. Meteorol Atmos Phys 112: 81–90.

Kyoung MS, Kim HS, Sivakumar B, Singh VP, Ahn KS (2011). Dynamic characteristics of monthly rainfall in the Korean Peninsula under climate change. Stoch Environ Res Risk Assess 25: 613–625.

Lee KH, Park JH (2008). Calibration of the Hargreaves Equation for the reference evapotranspiration estimation on a nation-wide scale. KSCE Journal of Civil Engineering 28: 675–681.

Li ZL, Li ZJ, Xu ZX, Zhou X (2013). Temporal variations of reference evapotranspiration in Heihe River basin of China. Hydrol Res 44: 904–916.

McCuen RH (1974). A sensitivity and error analysis of procedures used for estimating evaporation. Water Resour Bull 10: 486–498.

Moret D, Braud I, Arrue JL (2007). Water balance simulation of a dryland soil during fallow under conventional and conservation tillage in semiarid Aragon, Northeast Spain. Soil Till Res 92: 251–263.

Ngongondo C, Xu CY, Tallaksen LM, Alemaw B (2013). Evaluation of the FAO Penman-Monteith, Priestly-Taylor and Hargreaves models for estimating reference evapotranspiration in southern Malawi. Hydrol Res 44: 706–722.

Oh YG, Yoo SH, Lee SH, Choi JY (2011). Prediction of paddy field change based on climate change scenarios using the CLUE model. Paddy Water Environ 9: 309–323.

Onder D, Aydin M, Onder S (2009). Estimation of actual soil evaporation using E-DiGOR model in different parts of Turkey. Afr J Agric Res 4: 505–510.

Rim CS (2008). Trends of annual and monthly FAO Penman-Monteith reference evapotranspiration. KSCE Journal of Civil Engineering 28: 65–77.

Rim CS (2010). Evaluation of urban effects on trends of hydrometeorological variables. KSCE Journal of Civil Engineering 30: 71–80.

Romano E, Giudici M (2009). On the use of meteorological data to assess the evaporation from a bare soil. J Hydrol 372: 30–40.

Saxton KE (1975). Sensitivity analysis of the combination evapotranspiration equation. Agric Meteorol 15: 343–353.

Tabari H, Hosseinzadeh-Talaee P (2014). Sensitivity of evapotranspiration to climatic change in different climates. Global Planet Change 115: 16–23.

Terink W, Immerzeel WW, Droogers P (2013). Climate change projections of precipitation and reference evapotranspiration for the Middle East and Northern Africa until 2050. Int J Climatol 33: 3055–3072.

UNESCO (1979). Map of the World Distribution of Arid Regions. MAB Technical Note 7. Paris, France: UNESCO.

Van Dam JC, Huygen J, Wesseling JG, Feddes RA, Kabat P, van Walsum PEV, Groendijk P, van Diepen CA (1997). Theory of SWAP Version 2.0. Simulation of Water Flow, Solute Transport and Plant Growth in the Soil–Water–Atmosphere–Plant Environment. Technical Document 45, DLO Winand Staring Centre, Report 71. Wageningen, the Netherlands: Department of Water Resources, Agricultural University of Wageningen.

Vanderborght J, Graf A, Steenpass C, Scharnagl B, Prolingheuer N, Herbst M, Franssen HJH, Vereecken H (2010). Within-field variability of bare soil evaporation derived from Eddy Covariance measurements. Vadose Zone J 9: 943–954.

Wallace JS, Jackson NA, Ong CK (1999) Modelling soil evaporation in an agroforestry system in Kenya. Agric For Meteorol 94: 189–202.

Wang W, Peng S, Yang T, Shao Q, Xu J, Xing W (2011). Spatial and temporal characteristics of reference evapotranspiration trends in the Haihe River basin, China. J Hydrol Eng 16: 239–252.

Wang W, Shao Q, Peng S, Xing W, Yang T, Luo Y, Yong B, Xu J (2012). Reference evapotranspiration change and the causes across the Yellow River Basin during 1957-2008 and their spatial and seasonal differences. Water Resour Res 48: W05530.

Wang W, Xing W, Shao Q, Yu Z, Peng S, Yang T, Yong B, Taylor J, Singh VP (2013). Changes in reference evapotranspiration across the Tibetan Plateau: Observations and future projections based on statistical downscaling. J Geophys Res-Atmos 118: 4049–4068.

Wolfe SA (1997). Impact of increased aridity on sand dune activity in the Canadian Prairies. J Arid Environ 36: 421–432.

Xiao X, Horton R, Sauer TJ, Heitman JL, Ren T (2011). Cumulative soil water evaporation as a function of depth and time. Vadose Zone J 10: 1016–1022.

Xie H, Zhu X (2013). Reference evapotranspiration trends and their sensitivity to climatic change on the Tibetan Plateau (1970-2009). Hydrol Process 27: 3685–3693.

Xing W, Wang W, Shao Q, Peng S, Yu Z, Yong B, Taylor J (2014). Changes of reference evapotranspiration in the Haihe River Basin: Present observations and future projection from climatic variables through multi-model ensemble. Global Planet Change 115: 1–15.

Xu YP, Pal SL, Fu GT, Tian Y, Zhang XJ (2014). Future potential evapotranspiration changes and contribution analysis in Zhejiang Province, East China. J Geophys Res-Atmos 119: 2174–2192.

Yoo SH, Choi JY, Nam WH, Hong E (2012). Analysis of design water requirement of paddy rice using frequency analysis affected by climate change in South Korea. Agric Water Manage 112: 33–42.

Appendix A

The physical variables in Eq. (1) were calculated following Allen et al. (1994). On the other hand, the quantity δ can be written as:

$$\delta = e_s - e_a = e_s - e_s \frac{H}{100} = e_s(1 - \frac{H}{100}), \quad \text{(A1)}$$

where e_s, e_a, and H are the saturation vapor pressure (kPa), actual vapor pressure (kPa), and relative humidity (%), respectively.

The aerodynamic resistance r_a is related to the wind velocity logarithmic profile (Romano and Giudici, 2009). The shape of the wind logarithmic profile depends on both the zero plane displacement and the roughness height (Allen et al., 1994; van Dam et al., 1997):

$$r_a = \frac{\ln\left(\frac{z_m - d}{z_{om}}\right)\ln\left(\frac{z_h - d}{z_{oh}}\right)}{k^2 U_z}, \quad \text{(A2)}$$

where z_m is the height of the wind speed measurement (m), z_h is the height of the air temperature and humidity measurements (m), k is the von Karman constant (=0.41), U_z is the wind speed measurement at height z_m (m s^{-1}), d is the zero plane displacement of the wind profile, z_{zom} is the roughness parameter for momentum (m), and z_{zoh} is the roughness parameter for heat and water vapor (m). The d, z_{zom}, and z_{zoh} values are assessed as fractions of the vegetation height (h_c): $d = 2/3h_c$, $z_{zom} = 0.123h_c$, and $z_{zoh} = 0.1z_{zom} = 0.0123h_c$ (Allen et al., 1994).

Since we calculate bare soil evaporation, associated with the diameter of coarse sand, it was assigned as h_c = 0.1 cm (see van Dam et al., 1997, p. 72; Aydın and Polat, 2010). With a standardized height for wind speed, temperature, and humidity measurements at 2.0 m, and for a bare soil surface, the aerodynamic resistance for a 24-h time step is found as:

$$r_a = \frac{692.1}{u_2}. \tag{A3}$$

Here, u_2 is the wind speed (m s^{-1}) at 2.0 m height.

Appendix B

Based on the quotient rule for derivatives and Eq. (5), the derived formulas for the relative sensitivity coefficients (S) of the variables in Eq. (2) are as follows:

$$S_{R_n} = \frac{\partial E_p}{\partial R_n}.\frac{R_n}{E_p} = \frac{\Delta R_n}{\Delta(R_n - G_s) + 0.1248\rho c_p u_2 e_s (1 - \frac{H}{100})} \tag{B1}$$

$$S_{G_s} = \frac{\partial E_p}{\partial G_s}.\frac{G_s}{E_p} = \frac{-\Delta G_s}{\Delta(R_n - G_s) + 0.1248\rho c_p u_2 e_s (1 - \frac{H}{100})} \tag{B2}$$

$$S_H = \frac{\partial E_P}{\partial H}.\frac{H}{E_p} = \frac{-H/100}{\frac{\Delta(R_n - G_s)}{0.1248\rho c_p u_2 e_s} - \frac{H}{100} + 1} \tag{B3}$$

$$S_{u_2} = \frac{\partial E_p}{\partial u_2}.\frac{u_2}{E_p} = \frac{1}{\frac{\Delta(R_n - G_s)}{0.1248\rho c_p u_2 e_s (1 - \frac{H}{100})} + 1} \tag{B4}$$

Both Δ and δ are functions of the air temperature (T_a). The sensitivity function related to T_a can be approximated by (see McCuen, 1974):

$$\frac{dE_p}{dT_a} = \Delta \frac{dE_p}{d\delta} \,, \tag{B5}$$

$$S_{T_a} = \frac{\partial E_p}{\partial T_a} \cdot \frac{T_a}{E_p} = \frac{\Delta T_a}{\frac{\Delta (R_n - G_s)}{0.1248 \rho c_p u_2} + e_s (1 - \frac{H}{100})} \cdot \tag{B6}$$

Similarly, the derivative approach can be used to calculate the relative sensitivity coefficients ($^*S$) of the variables in Eq. (4):

$$^*S_{R_n} = \frac{\partial Et_O}{\partial R_n} \cdot \frac{R_n}{Et_O} = \frac{0.408 \Delta R_n}{0.408 \Delta R_n + \gamma \frac{900}{T_a + 273} u_2 e_s (1 - \frac{H}{100})} \,, \tag{B7}$$

$$^*S_H = \frac{\partial Et_O}{\partial H} \cdot \frac{H}{Et_O} = \frac{-H/100}{\frac{0.408 \Delta R_n}{\gamma \frac{900}{T_a + 273} u_2 e_s} - \frac{H}{100} + 1}, \tag{B8}$$

$$^*S_{u_2} = \frac{\partial Et_O}{\partial u_2} \cdot \frac{u_2}{Et_O} = \frac{1}{\frac{0.408 \Delta R_n}{\gamma \frac{900}{T_a + 273} u_2 e_s (1 - \frac{H}{100})} + 1} - \frac{0.34 u_2 \gamma}{\Delta + \gamma (1 + 0.34 u_2)}, \tag{B9}$$

$$^*S_{T_a} = \frac{\partial Et_O}{\partial T_a} \cdot \frac{T_a}{Et_O} = \frac{T_a \frac{df(T_a)}{dT_a}}{0.408 \Delta R_n + \gamma \frac{900}{T_a + 273} u_2 e_s (1 - \frac{H}{100})} - \frac{T_a \frac{dg(T_{a)}}{dT_a}}{\Delta + \gamma (1 + 0.34 u_2)}, \tag{B10}$$

where $\frac{df(T_a)}{dT_a}$ and $\frac{dg(T_a)}{dT_a}$ are the derivatives of the numerator and denominator of Eq. (4) with respect to air temperature (T_a), respectively, and are given in full in Appendix C.

Appendix C

In order to complete the sensitivity analysis of the FAO56-PM equation (Eq. (4)), it is necessary to calculate the following:

Assuming that G_s in Eq. (4) is zero for the daily scale, and R_n, γ, u_2, and H are constants, let:

$$f(T_a) = 0.408\Delta R_n + \gamma \frac{900}{T_a + 273} u_2 e_s (1 - \frac{H}{100}) \quad \text{(C1)}$$

and

$$g(T_a) = \Delta + \gamma(1 + 0.34u_2). \quad \text{(C2)}$$

Since Et_O is also a function of T_a:

$$\frac{\partial Et_O}{\partial T_a} = \frac{f'(T_a)g(T_a) - f(T_a)g'(T_a)}{\left[g(T_a)\right]^2} \quad , \quad \text{(C3)}$$

where $f'(T_a) = \frac{df(T_a)}{dT_a}$, and $g'(T_a) = \frac{dg(T_a)}{dT_a}$.

Both e_s and Δ are functions of T_a:

$$e_s = 0.6108 \exp(\frac{17.27T_a}{T_a + 237.3}). \quad \text{(C4)}$$

Here, in order to simplify the derivative expressions, saturation vapor pressure is formulated as a function of mean air temperature, although the use of Eq. (C4) for daily computations may lead to some errors. The slope of the vapor pressure curve is also calculated using mean temperature (Allen et al., 1994; Goyal, 2004):

$$\Delta = \frac{2503.16\exp(\frac{17.27T_a}{T_a + 237.3})}{(T_a + 237.3)^2}. \quad \text{(C5)}$$

Thus:

$$\frac{df(T_a)}{dT_a} = 0.408R_n \frac{d\Delta}{dT_a} + \frac{(\gamma 900u_2(1-\frac{H}{100})\frac{de_s}{dT_a})(T_a+273) - (\gamma 900u_2 e_s(1-\frac{H}{100})(1)}{(T_a+273)^2}, \quad \text{(C6)}$$

$$\frac{df(T_a)}{dT_a} = \frac{1021.29R_n(4098.17e^{\frac{17.27T_a}{T_a+237.3}} - 2(T_a+237.3)e^{\frac{17.27T_a}{T_a+237.3}})}{(T_a+237.3)^4} \quad \text{(C7)}$$
$$+ \frac{549.72\gamma(1-\frac{H}{100})u_2(\frac{4098.17(T_a+273)e^{\frac{17.27T_a}{T_a+237.3}}}{(T_a+237.3)^2} - e^{\frac{17.27T_a}{T_a+237.3}})}{(T_a+273)^2}$$

Similarly,

$$\frac{dg(T_a)}{dT_a} = \frac{d\Delta}{dT_a} \quad \text{(C8)}$$

and

$$\frac{dg(T_a)}{dT_a} = \frac{2503.16(4098.17e^{\frac{17.27T_a}{T_a+237.3}} - 2(T_a+237.3)e^{\frac{17.27T_a}{T_a+237.3}})}{(T_a+237.3)^4}. \quad \text{(C9)}$$

Then $\frac{\partial Et_O}{\partial T_a}$ can be obtained by combining the above terms:

$$\frac{\partial Et_O}{\partial T_a} = \frac{\frac{df(T_a)}{dT_a}(\Delta + \gamma(1+0.34u_2)) - (0.408\nabla R_n + \gamma\frac{900}{T_a+273}u_2 e_s(1-\frac{H}{100}))\frac{dg(T_a)}{dT_a}}{(\Delta+\gamma(1+0.34u_2))^2}. \quad \text{(C10)}$$

Finally, the relative sensitivity function related to T_a is found, as given in Eq. (B10).